SMARCAL1 maintains telomere integrity during DNA replication

Lisa A. Poole[a], Runxiang Zhao[a], Gloria G. Glick[a], Courtney A. Lovejoy[a], Christine M. Eischen[b], and David Cortez[a,1]

[a]Department of Biochemistry, Vanderbilt University School of Medicine, Nashville, TN 37027; and [b]Department of Pathology, Microbiology, and Immunology, Vanderbilt University School of Medicine, Nashville, TN 37027

Edited by Philip C. Hanawalt, Stanford University, Stanford, CA, and approved October 29, 2015 (received for review June 1, 2015)

The SMARCAL1 (SWI/SNF related, matrix-associated, actin-dependent, regulator of chromatin, subfamily A-like 1) DNA translocase is one of several related enzymes, including ZRANB3 (zinc finger, RAN-binding domain containing 3) and HLTF (helicase-like transcription factor), that are recruited to stalled replication forks to promote repair and restart replication. These enzymes can perform similar biochemical reactions such as fork reversal; however, genetic studies indicate they must have unique cellular activities. Here, we present data showing that SMARCAL1 has an important function at telomeres, which present an endogenous source of replication stress. SMARCAL1-deficient cells accumulate telomere-associated DNA damage and have greatly elevated levels of extrachromosomal telomere DNA (C-circles). Although these telomere phenotypes are often found in tumor cells using the alternative lengthening of telomeres (ALT) pathway for telomere elongation, SMARCAL1 deficiency does not yield other ALT phenotypes such as elevated telomere recombination. The activity of SMARCAL1 at telomeres can be separated from its genome-maintenance activity in bulk chromosomal replication because it does not require interaction with replication protein A. Finally, this telomere-maintenance function is not shared by ZRANB3 or HLTF. Our results provide the first identification, to our knowledge, of an endogenous source of replication stress that requires SMARCAL1 for resolution and define differences between members of this class of replication fork-repair enzymes.

SMARCAL1 | telomere | replication stress | c-circle

The complete and accurate duplication of the genome in each cell-division cycle is challenged by many sources of replication stress including DNA template damage, collisions between replication and transcriptional machineries, and difficult-to-replicate DNA sequences. To overcome these challenges, cells use a multifaceted replication stress response that includes specialized enzymes that stabilize, repair, and restart stalled replication forks.

Among these enzymes are members of the SNF2 family of DNA-dependent ATPases that include SMARCAL1 (SWI/SNF related, matrix-associated, actin-dependent, regulator of chromatin, subfamily A-like 1), ZRANB3 (zinc finger, RAN-binding domain containing 3), and HLTF (helicase-like transcription factor) (1). These DNA translocases bind replication fork structures, hydrolyze ATP, and perform branch migration reactions (2–11). Each of these enzymes can catalyze fork regression in vitro, although it is still unclear whether they perform this reaction in vivo (3, 4, 6–8, 11, 12). SMARCAL1 and ZRANB3 also can catalyze DNA strand annealing, disrupt displacement loop structures, and catalyze fork restoration reactions to return a regressed fork back into a normal fork structure (3, 4, 13).

Given the overlapping biochemical activities among these translocases, it is unclear why the cell employs so many different enzymes at stalled forks. Genetic studies indicate these proteins have distinct functions. HLTF knockdown results in a decrease in cell viability following treatment with UV and the methylating agent methyl methanesulfonate (MMS) (6, 7, 14). Similarly, ZRANB3 depletion sensitizes cells to MMS. ZRANB3-deficient cells also are sensitive to the topoisomerase I inhibitor camptothecin, the DNA cross-linker mitomycin C (MMC), the ribonucleotide reductase inhibitor hydroxyurea (HU), the interstrand cross-linking agent cisplatin, and ionizing radiation (4, 10, 15, 16). Furthermore, ZRANB3 knockdown results in an increased rate of sister chromatid exchanges (SCEs) that is exacerbated by treatment with DNA-damaging agents (4). SMARCAL1 depletion also sensitizes cells to similar genotoxic agents including HU, MMC, and camptothecin, but SMARCAL1-deficient cells do not have an increased frequency of SCEs (2, 17–19). Inherited mutations in *SMARCAL1* cause Schimke immunoosseous dysplasia (SIOD), a disease characterized by renal failure, growth defects, immune deficiencies, and a predisposition to cancer (20–22).

Biochemical studies suggest these enzymes do have some degree of specificity dictated by both intrinsic differences in substrate recognition and differences in protein interaction partners and regulation. SMARCAL1, ZRANB3, and HLTF all have an SNF2-type ATPase domain but differ in the accessory domains needed for DNA binding and activity. A HARP domain in SMARCAL1 is thought to mediate structure-specific DNA binding, whereas a HIRAN domain in HLTF recognizes the 3′ end of DNA strands (3, 12, 23). High-resolution structures indicate that these domains are distinct even though biochemically they both may serve to link the ATPase motor domains to specific substrates and reactions (12, 24). As yet, the structure of the ZRANB3 accessory domain is unknown, although it has been postulated to resemble a HARP domain (10).

SMARCAL1 also is unique among these enzymes for its ability to bind directly to replication protein A (RPA) (2, 5, 17, 18). This interaction not only recruits SMARCAL1 to replication forks but also regulates its enzymatic activity. Specifically, the location of RPA binding to replication fork structures can variably inhibit or activate SMARCAL1 (13, 25). RPA binding is critical for at least some of the replication stress-response functions of SMARCAL1 in cells (2, 5, 17, 19).

Significance

DNA replication is challenged by many sources of stress including DNA damage and difficult-to-replicate DNA sequences. Several related replication fork remodeling enzymes including SMARCAL1 (SWI/SNF related, matrix-associated, actin-dependent, regulator of chromatin, subfamily A-like 1) respond to this replication stress to ensure complete and accurate DNA synthesis. Here we describe telomere DNA sequences as the first endogenous source of replication stress that SMARCAL1 is required to resolve. This telomere replication function is not shared by highly related enzymes and is genetically separable from other SMARCAL1 activities in bulk chromosomal replication. We identify a previously unknown function of SMARCAL1 that could contribute to the phenotypes associated with Schimke immunoosseous dysplasia, a human disease caused by *SMARCAL1* mutations.

Author contributions: L.A.P. and D.C. designed research; L.A.P., R.Z., and G.G.G. performed research; C.A.L. and C.M.E. contributed new reagents/analytic tools; L.A.P., C.A.L., and D.C. analyzed data; and L.A.P. and D.C. wrote the paper.

The authors declare no conflict of interest.

This article is a PNAS Direct Submission.

[1]To whom correspondence should be addressed. Email: david.cortez@vanderbilt.edu.

This article contains supporting information online at www.pnas.org/lookup/suppl/doi:10.1073/pnas.1510750112/-/DCSupplemental.

These differences point toward unique functions of these enzymes, perhaps responding to unique types of replication stress. Although experimental analyses have focused largely on their responses to added genotoxic agents, it is clear that they are needed for endogenous replication problems as well. For example, knockdown of SMARCAL1 causes increased DNA damage in otherwise unperturbed S-phase cells (2, 17, 19, 26). Defining which endogenous replication stresses are resolved by each enzyme will be critical to understanding their functions in vivo. One source of endogenous replication stress is the TTAGGG repeats of telomeric DNA. Telomeres present challenges to the replication machinery because they are capable of forming unusual DNA structures (27). Because they also are origin-poor regions, it is especially important to prevent replication fork inactivation within telomeric sequences (28).

In this study we find that SMARCAL1, but not ZRANB3 or HLTF, is needed for successful replication through telomere sequences. These results demonstrate functional differences among these fork-repair proteins and identify the first (to our knowledge) endogenous source of replication stress that requires SMARCAL1 activity for resolution.

Results

SMARCAL1 Is Required to Prevent the Accumulation of DNA Damage at Telomeres. Depleting SMARCAL1 from human cells causes an increased basal level of DNA damage in S-phase cells without the addition of exogenous genotoxic agents (2, 17, 19, 26). We reasoned that this replication-associated genome instability may reflect a requirement for SMARCAL1 to respond to endogenous forms of replication stress such as difficult-to-replicate sequences. Telomeres present one source of such replication stress because of their propensity to form structures such as G-quadruplexes (29) and t-loops (30). Therefore we tested whether SMARCAL1 is required to maintain genome integrity specifically within telomere sequences.

First, we examined whether the increased DNA damage caused by SMARCAL1 depletion included telomere damage. Indeed, SMARCAL1 knockdown caused a significant increase in telomere dysfunction-induced foci (TIFs), as indicated by the colocalization of 53BP1 and telomeric DNA (Fig. 1 *A* and *B*), and a significant increase in colocalization of RPA with telomeres (Fig. 1 *C–E*). The amount of telomere damage is relatively small compared with that caused by the inactivation of shelterin proteins (28, 31), suggesting that the damage may be either transient or confined to a small subset of telomeres. These telomeric defects are not the result of off-target effects of the siRNA, because an siRNA-resistant WT SMARCAL1 cDNA is capable of complementing the siRNA-transfected cells (Fig. 1 *C–E*).

RPA regulates SMARCAL1 but typically is excluded from functional telomeres (32). Therefore, we tested if an RPA-binding–deficient SMARCAL1 mutant (ΔN) also could rescue the increased incidence of RPA–telomere colocalization. This SMARCAL1 mutant lacks 32 amino acids at the N terminus of SMARCAL1 that directly binds the 32C domain of RPA and is required for SMARCAL1 localization to replication forks stalled by HU (2). Surprisingly, we also observed a significant reduction in the frequency of TIFs in cells expressing Δ*N*-SMARCAL1 (Fig. 1 *C–E*). The level of expression is approximately twofold higher than that of endogenous SMARCAL (Fig. 1*E*). This level of Δ*N*-SMARCAL1 expression is not capable of rescuing other SMARCAL1 loss-of-function phenotypes (2, 5, 17, 19, 26). Thus, the function of SMARCAL1 at telomeres may be separable from its function in bulk chromosomal replication stress responses, as discussed below.

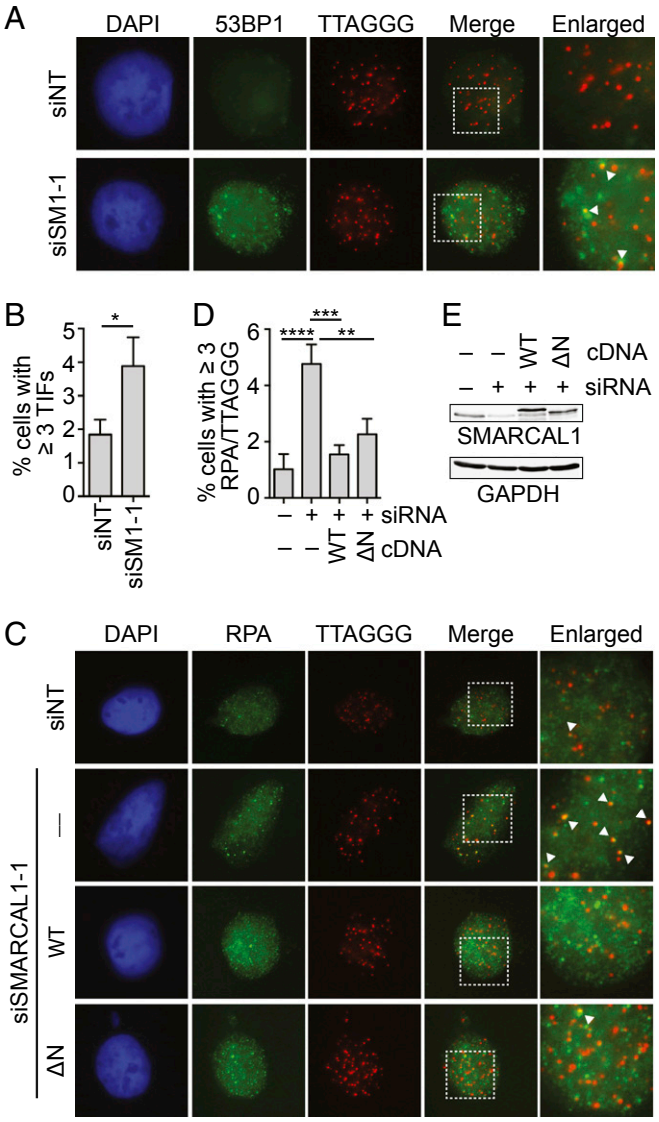

Fig. 1. SMARCAL1 silencing causes telomere DNA damage. HeLa1.3 cells were transfected with nontargeting (NT) or SMARCAL1 (SM1-1) siRNA and were fixed, and IF-FISH was performed with 53BP1 or RPA antibodies and a telomeric DNA probe, as indicated. (*A*) Representative images of TIFs in SMARCAL1-depleted HeLa1.3 cells. White arrowheads indicate colocalization between 53BP1 and telomeres (TIFs). (*B*) Quantification of cells with three or more TIFs. Samples were compared with a two-tailed Student's *t*-test ($P = 0.02$). (*C–E*) HeLa1.3 cells and cells expressing siRNA-resistant WT SMARCAL1 or RPA-interaction–deficient SMARCAL1 (ΔN) were transfected with the indicated siRNAs and imaged for RPA and telomere localization. (*C*) Representative images of RPA–telomere colocalization. (*D*) Quantification of cells with three or more RPA/telomere colocalized foci. Samples were compared with one-way ANOVA ($P = 0.0001$). Bonferroni's multiple comparison test was used as a follow-up to compare siSMARCAL1 with siNT and complemented samples. (*E*) Immunoblot to monitor SMARCAL1 expression. Plots in *B* and *D* are mean ± SD from three independent experiments in which ∼100 and 500 nuclei were examined, respectively.

SMARCAL1 Depletion Causes the Accumulation of Circular Extrachromosomal Telomere DNA. The increase in TIFs in SMARCAL1-deficient cells suggests that SMARCAL1 maintains telomere integrity. To characterize this function further, we examined whether SMARCAL1 deficiency caused additional telomere dysfunction phenotypes. Indeed, silencing SMARCAL1 in HeLa1.3 cells caused a significant increase in the abundance of extrachromosomal, partly duplexed, circular DNAs derived from telomere sequences (C-circles) (Fig. 2*A*). The abundance of these C-circles correlated with the degree of SMARCAL1 knockdown, although C-circle abundance was not as high as that seen in U2OS cells that use a recombination-based mechanism of telomere maintenance. The C-circles were resistant to degradation by exonuclease V, a nuclease that selectively digests linear DNA, and were dependent on rolling circle amplification by phi29 DNA polymerase. We also observed an elevated level of C-circles in

CELL BIOLOGY

SMARCAL1-deficient (*Smarcal1*$^{\Delta/\Delta}$) mouse embryonic fibroblasts (MEFs) compared with MEFs derived from WT littermates (Fig. 2*B*).

Expression of human GFP-SMARCAL1 in the *Smarcal1*$^{\Delta/\Delta}$ MEFs returned C-circle abundance to low levels (Fig. 2*C*). However, an SIOD patient-derived SMARCAL1 mutant protein (R764Q) that lacks enzymatic activity did not decrease C-circle abundance (Fig. 2*C*). These data indicate that, like the genome-wide function of SMARCAL1, its function at telomeres also requires hydrolysis of ATP. The N-terminal truncation mutant of SMARCAL1 that removes the RPA-binding domain (ΔN) also prevented the accumulation of C-circles, again suggesting a separation of SMARCAL1 functions at telomeres from other sites of replication stress (Fig. 2*C*). Similar results were also obtained with siRNA to SMARCAL1 in HeLa1.3 cells complemented WT-, R764Q-, and ΔN-SMARCAL1 (Fig. 2*D*). Thus, we conclude that the function of SMARCAL1 at telomeres is dependent on its enzymatic activity but does not require an interaction with RPA.

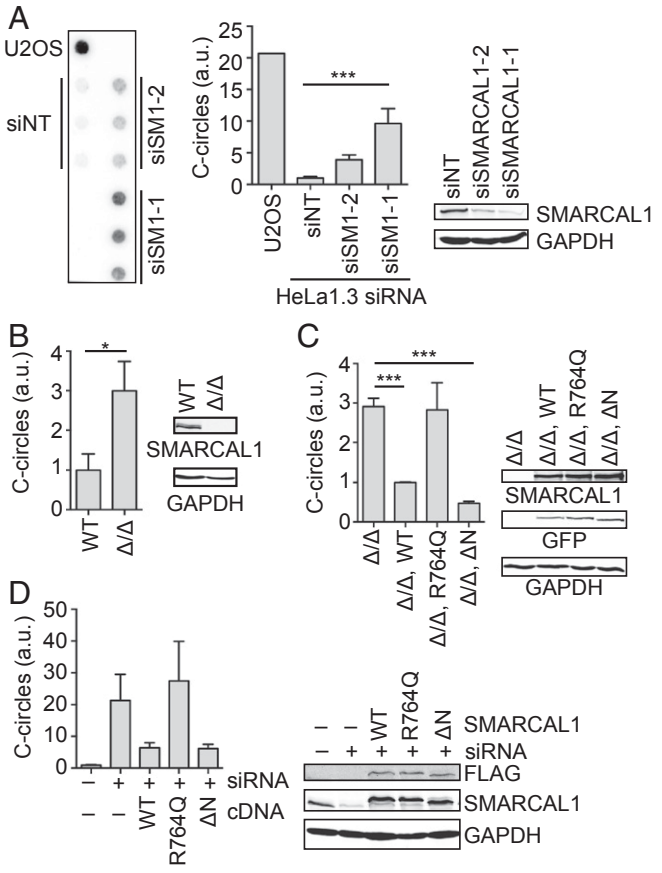

Fig. 2. SMARCAL1 deficiency causes the accumulation of extrachromosomal telomere circles. (*A*) C-circles were quantified from genomic DNA isolated from untransfected U2OS cells and HeLa1.3 cells transfected with the indicated siRNAs. (*Left*) A representative dot blot is shown. (*Center*) Values were normalized so that siNT was set at 1. Samples were compared with one-way ANOVA ($P < 0.0001$). Bonferroni's multiple comparison test was used as a follow-up to compare siNT with siSMARCAL1 samples. (*Right*) Immunoblot analysis of SMARCAL1 protein expression in HeLa1.3 cells. (*B*) Quantification of C-circles from *Smarcal1*$^{\Delta/\Delta}$ vs. WT MEFs. Values were normalized so that WT was set at 1. Samples were compared with two-tailed Student's *t*-test ($P = 0.015$). a.u, arbitrary units. (*C*, *Left*) Quantification of the C-circle assay performed in *Smarcal1*$^{\Delta/\Delta}$ MEFs complemented with GFP-tagged WT, ATPase-dead (R764Q), and RPA-binding–deficient (ΔN) SMARCAL1. Values were normalized so that Δ/Δ,WT was set at 1. Error bars indicate the SD from three experiments. Samples were compared with one-way ANOVA ($P < 0.001$) followed by Bonferroni's multiple comparison test to compare Δ/Δ with complemented samples. (*Right*) Immunoblot analysis of SMARCAL1 expression. (*D*, *Left*) Quantification of C-circles in complemented HeLa1.3 cells treated with SMARCAL1-1 siRNA. Samples were compared with one-way ANOVA ($P = 0.01$). Error bars in panels indicate the SEM from at least three experiments. (*Right*) Immunoblot analysis of SMARCAL1 expression.

SMARCAL1 Functions During Replication Elongation to Prevent SLX4-Dependent Telomere Processing. Previous studies investigating the origin of C-circles demonstrated that ongoing replication is a requirement for C-circle formation in ALT cells (33). We performed C-circle assays on samples treated with the replication-stalling agents HU or aphidicolin to investigate the dependence on replication in a SMARCAL1-depleted setting. C-circle levels in SMARCAL1-deficient cells were reduced to baseline levels similar to those of samples treated with nontargeting siRNA after treatment with either replication stress agent for 48 h (Fig. 3*A*). Thus, although SMARCAL1 is recruited to stalled forks in response to HU and aphidicolin, it is not required to prevent extrachromosomal telomere circles when replication elongation is inhibited by these drugs.

In addition to replication, extrachromosomal telomere circle accumulation is also dependent on the function of the nuclease scaffold protein SLX4, in at least some settings (34). To test whether SLX4 is required to generate the C-circles in SMARCAL1-deficient cells, we codepleted SMARCAL1 and SLX4 in HeLa1.3 cells using siRNA. Although we were able to silence SLX4 expression only partly, we did observe an ∼50% decrease in C-circles (Fig. 3*B*). Therefore, we conclude that the C-circles generated in SMARCAL1-deficient cells are generated at least partly through telomere cleavage by an SLX4-dependent nuclease during DNA replication.

The SMARCAL1 Function at Telomeres Is Not Shared by Related DNA Translocases. We next asked whether the telomere function of SMARCAL1 is shared by related DNA translocases, including HLTF and ZRANB3. In contrast to SMARCAL1, depletion of either ZRANB3 or HLTF from HeLa1.3 cells did not cause any change in C-circle levels (Fig. 3 *C* and *D*). We also did not observe any increase in C-circle abundance when we knocked down the RECQ helicases WRN or BLM (Fig. 3 *C* and *D*). Thus, although these enzymes are all recruited to stalled replication forks and are capable of catalyzing overlapping biochemical reactions such as fork reversal, only SMARCAL1 loss of function causes increased telomere C-circle abundance.

Telomere Length and Recombination in SMARCAL1-Deficient Settings. C-circles have been described previously as a marker of cells using the ALT pathway for telomere elongation, which involves a recombination mechanism (35). In addition to C-circles and damage at telomeres, ALT cells also display other changes in telomere integrity including increased rates of telomere recombination and dramatic changes in telomere length.

Because we saw damage at telomeres and C-circles, we next examined if there is a change in telomere length in SMARCAL1-deficient MEFs. By telomere restriction fragment analysis, we saw a small but not statistically significant difference in telomere length in *Smarcal1*$^{\Delta/\Delta}$ MEFs compared with WT littermates (Fig. 4 *A* and *B*). There also was no significant difference in telomere lengths in HeLa1.3 cells depleted of SMARCAL1 with siRNA for 3 weeks (Fig. 4*C*).

We also examined if SMARCAL1 depletion affected telomere recombination rates, another hallmark of ALT. We did not observe a significant increase in the frequency of telomere SCES (t-SCEs) using chromosome orientation FISH on metaphase spreads from HeLa1.3 cells depleted of SMARCAL1 (Fig. 4*D*). As a control, we did find that depletion of ASF1 caused a significant increase in t-SCEs, as reported previously (Fig. 4*D*) (33). Additionally, we did not observe a significant change in the percentage of telomeres with multiple telomere signals (MTS) or telomere signal free ends in SMARCAL1-depleted cells (Fig. 4*D*). Similarly, no significant differences in t-SCE, MTS, or missing telomere frequencies were observed between WT and *Smarcal1*$^{\Delta/\Delta}$ MEFs (Fig. 4*E*).

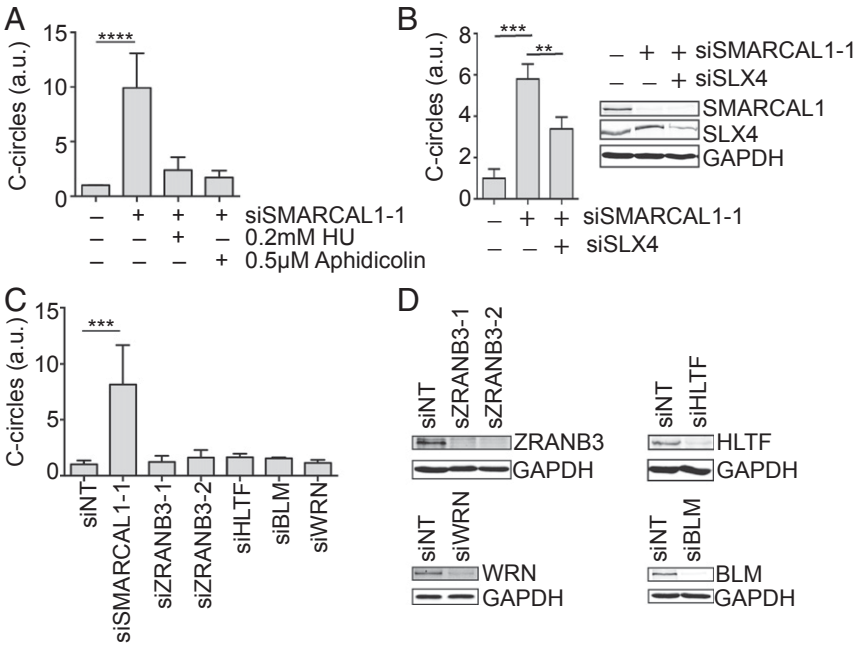

Fig. 3. Replication-dependent C-circle formation is specific to SMARCAL1 deficiency. (*A*) HeLa1.3 cells were transfected with NT or SMARCAL1 siRNA and were treated with 0.2 mM HU or 0.5 μM aphidicolin for 48 h before C-circle abundance was assessed. (*B* and *C*) Quantification of C-circles after transfection of HeLa1.3 cells with the indicated siRNAs. Values were normalized so that siNT was set at 1. Error bars in all panels are SD from three experiments. Samples were compared with one-way ANOVA (*A*, $P < 0.0001$; *B*, $P = 0.0002$; *C*, $P < 0.001$) followed by Bonferroni's multiple comparison test to compare siNT with other siRNA transfection samples. (*D*) Immunoblots to monitor ZRANB3, HLTF, BLM, and WRN expression.

Another recombination marker of ALT cells is an increased frequency of promyelocytic leukemia (PML) colocalization with telomeric DNA. These ALT-associated PML bodies (APBs) also include homologous recombination proteins, which may coordinate these components to facilitate recombination events at telomeres (36). SMARCAL1 depletion in HeLa1.3 cells does not cause a significant increase in the colocalization of telomeric DNA and PML protein, despite an increase in total number of PML foci (Fig. S1). Therefore, SMARCAL1 loss is not sufficient to induce telomere recruitment to these proposed recombination centers. In contrast, almost 100% of the ALT$^+$ U2OS cells display colocalization of TTAGGG sequences with PML (Fig. S1).

Given the lack of many ALT phenotypes in telomerase-positive HeLa cells following SMARCAL1 depletion, we proceeded to examine whether SMARCAL1 deficiency altered telomere integrity in an ALT$^+$ cell line. Following SMARCAL1 knockdown in ALT$^+$ U2OS cells, we quantified the frequency of TIFs, APBs, and RPA colocalization with telomeres in SMARCAL1-proficient and -deficient settings. In all cases, loss of SMARCAL1 in U2OS cells had no significant effect on the frequency of the occurrence of each marker of telomere instability (Fig. S2 *A*–*F*). Additionally, there was no difference in the abundance of C-circles between U2OS cells treated with nontargeting or SMARCAL1 siRNA (Fig. S2*G*).

SMARCAL1 Localization to Telomeres. SMARCAL1 function in genome-wide replication is thought to be the result of direct activity at replication forks, requiring RPA-dependent localization to sites of replication stress (2, 3, 5, 17, 18). To test whether SMARCAL1 also localizes to telomeres and directly functions to promote telomere integrity during DNA replication, we performed telomere immunofluorescence (IF)-FISH and telomere ChIP. When GFP-SMARCAL1 is highly overexpressed in U2OS cells, we are able to see a subset of SMARCAL1 foci colocalize with the telomere probe (Fig. S3*A*). However, in these circumstances, high levels of overexpressed SMARCAL1 induce DNA damage during DNA

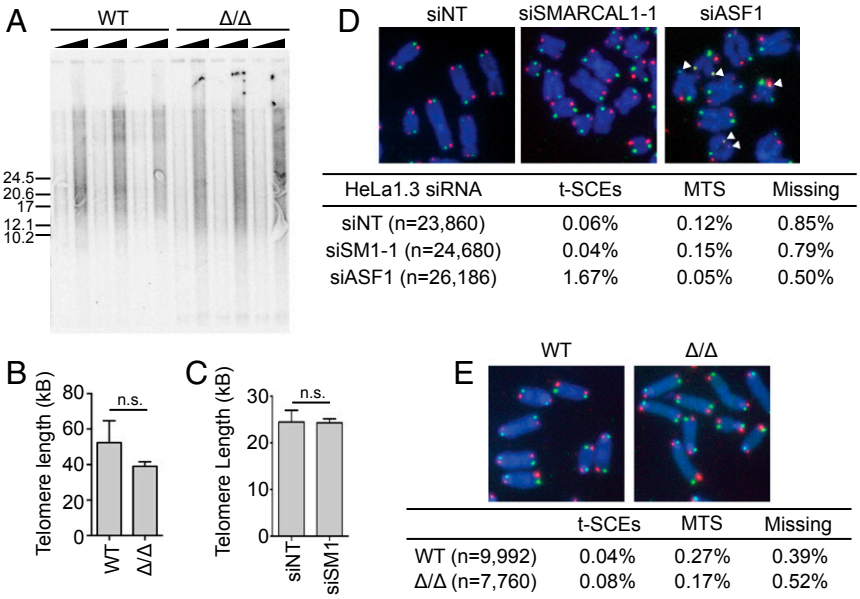

HeLa1.3 siRNA	t-SCEs	MTS	Missing
siNT (n=23,860)	0.06%	0.12%	0.85%
siSM1-1 (n=24,680)	0.04%	0.15%	0.79%
siASF1 (n=26,186)	1.67%	0.05%	0.50%

	t-SCEs	MTS	Missing
WT (n=9,992)	0.04%	0.27%	0.39%
Δ/Δ (n=7,760)	0.08%	0.17%	0.52%

Fig. 4. Analysis of telomere length and recombination in SMARCAL1-deficient cells. (*A*–*C*) Telomere length was analyzed by analysis of telomere restriction fragments in SMARCAL1 WT and Δ/Δ MEFs or HeLa1.3 cells transfected with nontargeting or SMARCAL1 siRNA every 3 d for a total of seven transfections. Two quantities of telomere DNA for each of three independent samples were separated by pulse-field gel electrophoresis before Southern blotting. Error bars indicate SD. Significance (MEFs, $P = 0.14$; HeLa1.3, $P = 0.9$) was determined using two-tailed Student's *t*-test. (*D* and *E*) Metaphase spreads from HeLa1.3 cells transfected with NT, SMARCAL1, or ASF1 siRNA (*D*) or SMARCAL1 WT and Δ/Δ MEFs (*E*) were fixed and stained with telomere probes to the G-rich repeat (red) and the C-rich repeat (green). Representative images are shown. White arrowheads indicate t-SCE events. Tables depict the mean frequency of t-SCEs, MTS, and signal-free ends (Missing) (n = number of telomere ends analyzed).

CELL BIOLOGY

replication (2). When SMARCAL1 from an alternative vector that does not cause DNA damage was expressed at lower levels, no specific SMARCAL1 localization at telomeres was evident in either U2OS or Hela1.3 cells (Fig. S3*A*). Furthermore, when we performed telomere ChIP in HeLa1.3 cells stably expressing Flag-HA-WT SMARCAL1, we were unable to see an enrichment of telomere DNA immunoprecipitated with SMARCAL1 compared with a control ChIP sample (Fig. S3 *B–D*). Conversely, the shelterin protein POT1 was significantly enriched (Fig. S3 *C–E*). Thus, SMARCAL1 can associate with telomeres; however, it is not detectable when expressed at nearly endogenous levels, suggesting a transient association, perhaps with only a subset of telomeres within the cell population undergoing replication.

Discussion

Despite the utility of genotoxic agents in studying the replication stress response, these drugs often fail to differentiate the functions of related fork-repair enzymes and are assumed to model some undefined, endogenous source of replication stress. In the current study, we show that SMARCAL1 has a unique function in promoting replication through an endogenous source of replication stress—telomeric sequences. To our knowledge, this is the first identification of an endogenous source of replication stress that is resolved by SMARCAL1 (or any of the related enzymes).

Following SMARCAL1 inactivation, cells display markers of telomere instability including TIF formation and the accumulation of extrachromosomal, circular telomeric DNA (C-circles). Notably, we did not observe the generation of C-circles after inactivation of the related enzymes ZRANB3 and HLTF. Although all three enzymes possess similar DNA-remodeling capabilities in vitro, our studies provide a distinction among these DNA translocases in cells.

There are many additional repair enzymes, including helicases such as WRN, BLM, and RTEL1, that work at damaged replication forks to promote genome stability. WRN likely has a function at telomeres and can form a complex with SMARCAL1 (37); however, WRN knockdown did not cause C-circle formation. RTEL1 has at least two essential telomere functions, although we have not detected any interaction between RTEL1 and SMARCAL1 (34, 38). It will be important to understand how these helicases work cooperatively to achieve successful telomere replication.

Our discovery that SMARCAL1 has an important function in telomere stability provides the first evidence, to our knowledge, of a specific requirement of SMARCAL1 at a site of endogenous replication stress. However, the damage that occurs following knockdown of SMARCAL1 does not occur exclusively at telomeres. Furthermore, a separation-of-function SMARCAL1 mutant (ΔN) indicates that the SMARCAL1 function at telomeres is separable from its activity during bulk chromosomal replication or in response to exogenous genotoxic drugs. The nature of the other types of replication stress remains to be identified, although the biochemical data suggest it may be specific to problems in leading-strand replication (13, 25).

SMARCAL1-Deficient Cells Display a Telomere Instability Phenotype Partially Reminiscent of the ALT Pathway. C-circles have been described previously as a marker of cells using the ALT pathway for telomere maintenance (39). Surprisingly, although SMARCAL1 depletion causes C-circle formation, we did not observe other ALT-related phenotypes. Specifically, we did not observe increased rates of intertelomere recombination, colocalization of telomeric DNA with PML, or dramatic changes in telomere length in SMARCAL1-deficient cells (Fig. 4 and Fig. S1). C-circles also have been seen following loss of the ASF1 histone chaperone, but in that case other ALT-like phenotypes were observed also (33). SMARCAL1 deficiency is insufficient to generate all ALT phenotypes, indicating that C-circle formation is not a sufficient indicator of ALT utilization. Likewise, SMARCAL1 depletion in the context of an ALT^+ cell line has no significant effect on telomere stability (TIFs and RPA/telomere colocalization), APB frequency, or C-circle abundance (Fig. S2), also indicating that SMARCAL1 is not necessary to maintain an ALT phenotype.

Although C-circles are a major hallmark of cells using the ALT pathway, it is unclear whether they are required for the recombination-based mechanism of telomere maintenance. As yet, it is unclear how C-circles are actually generated either in ALT or SMARCAL1-deficient cells, although an SLX4-dependent nuclease is involved in both. SLX4 scaffolds several endonucleases that can cleave stalled or damaged replication forks (40). Thus, it is likely that replication forks stalled within telomeric sequences undergo aberrant processing when SMARCAL1 is inactivated. Because we do not observe an increased rate of intertelomere recombination, it is possible the C-circles are formed as a result of intratelomere-processing events.

SMARCAL1 Bulk Chromatin and Telomere Functions Are Separable. Although RPA is required for SMARCAL1 function in bulk chromatin replication following the addition of a genotoxic agent, RPA binding is dispensable for SMARCAL1 function at telomeres. This result is intriguing but not entirely unexpected, because RPA typically is excluded from functional telomeres to prevent aberrant DNA damage response signaling (32).

This RPA independence raises the question of how SMARCAL1 localizes to sites of replication stress at telomeres. It is unclear if another protein is required to recruit SMARCAL1 to telomeres, although we have failed to find any direct interaction with known telomere-binding proteins. As an alternative to protein-mediated recruitment, SMARCAL1 could use its high-affinity DNA binding to localize to telomeres, because SMARCAL1 is capable of binding a variety of DNA structures with high affinity in the absence of RPA (3, 11, 41). We have been able to detect SMARCAL1 localization at telomeres only when it is highly overexpressed (Fig. S3). Thus, its localization to telomeres may occur only during the short window when telomere replication is happening. Alternatively, it is possible that SMARCAL1 exerts its telomere-maintenance function indirectly through some kind of signaling mechanism. We think this alternative is unlikely, because SMARCAL1's DNA-dependent ATPase activity is needed for its telomere-maintenance function. Finally, we cannot rule out the possibility that the twofold overexpression of the RPA-binding mutant of SMARCAL1 is able to overcome the requirement for RPA to localize to sites of replication stress at telomeres. However, this level of expression is unable to rescue other phenotypes associated with SMARCAL1 silencing, including increased intensity of the DNA damage marker γH2AX and defects in cell-cycle progression (2, 17).

Conclusions. To our knowledge, our data provide the first indication of an endogenous replication stress that SMARCAL1 acts to resolve. It also separates the function of SMARCAL1 from related fork-repair enzymes. SMARCAL1 deficiency causes the human disease SIOD. Symptoms associated with SIOD include renal failure, growth defects, immune deficiencies, and a predisposition to cancer (20–22). SMARCAL1 deficiency does not result in premature aging. However, it will be important to investigate whether some of the SIOD phenotypes are caused by the need for SMARCAL1 to promote the replication of telomeric DNA.

Experimental Procedures

Cell Culture. HeLa1.3 and U2OS cells were cultured in DMEM supplemented with FBS (10% and 7.5%, respectively). MEFs were generated from WT and *Smarcal1*$^{\Delta/\Delta}$ (22) embryos from the same pregnant female and were cultured as previously described (42). MEF generation from mice was completed as approved by the Vanderbilt Institutional Animal Care and Use Committee. *Smarcal1*$^{\Delta/\Delta}$ MEFs express a nonfunctional SMARCAL1 protein in which the first two exons of the mRNA transcript are deleted. siRNA transfections were performed with Lipofectamine RNAiMAX (Life Technologies) or Dharmafect 1 (Dharmacon). U2OS cells were transiently transfected with GFP-SMARCAL1 using Fugene HD (Promega).

MEFs were immortalized by infection with retroviral particles expressing SV40 large T antigen (pBABE-puro-SV40). HeLa1.3 cells were infected with retrovirus expressing WT, ATPase-dead (R764Q), RPA binding-deficient (ΔN) Flag-HA-SMARCAL1, or Flag-HA-POT1. Stable MEF cell lines were produced by lentiviral infection of GFP-SMARCAL1 WT, RQ, and ΔN constructs.

Antibodies and Reagents. Antibodies used for immunoblotting were as follows: SMARCAL1 (2); GFP (Clontech); WRN (Novus); ZRANB3 (Bethyl); GAPDH (Millipore); Flag M2 (Sigma); HA (Covance); HLTF (Karlene Cimprich, Stanford University, Stanford, CA); and SLX4 (Bethyl). Additional antibodies for immunofluorescence include PML (Santa Cruz), RPA2 (Abcam), and 53BP1 (Millipore). Antibodies for telomere ChIP include HA (Abcam) and Flag M2. Cy3-CCCTAA and Alexa488-TTAGGG telomere probes were purchased from PNA Bio.

C-Circle Assay. The C-circle assay was performed essentially as described previously (39).

IF-Telomere FISH. Cells were grown on coverslips and washed with PBS. Soluble protein was preextracted with 0.5% Triton X-100 in PBS for 5 min on ice, washed with PBS, and fixed with 3% PFA-2% (wt/vol) sucrose for 10 min. After washing and incubating with blocking solution [1 mg/mL BSA, 3% (vol/vol) goat serum, 0.1% Triton X-100, 1 mM EDTA, pH 8.0] for 30 min, the coverslips were incubated with primary and secondary antibodies, washed, fixed with 3% PFA–2% sucrose for 5 min, washed with PBS, and dehydrated in EtOH. Coverslips were covered with 50 μL of hybridizing solution [70% (vol/vol) formamide, 0.5% Roche blocking reagent diluted in 100 mM maleic acid, 150 mM NaCl (pH 7.5), and 10 mM Tris (pH 7.2) with 100 nM Cy3-CCCTAA probe] and were denatured for 3 min on a heat block set at 80 °C. After overnight hybridization, coverslips were washed twice for 15 min with 70% formamide and 10 mM Tris (pH 7.2) and three times with PBS. DAPI (170 ng/mL) was added in the second washing. Cells then were dehydrated and mounted on slides with Prolong Gold (Invitrogen).

Chromosome Orientation FISH. Cells were labeled with 7.5 mM BrdU and 2.5 mM BrdC for 16–20 h and were treated with 0.5 μg/mL of KaryoMAX colcemid (Life Technologies) for 2 h. Cells were harvested by trypsinization, incubated in 75 mM KCl at 37 °C for 15 min, and fixed overnight with 70% methanol:30% (vol/vol) glacial acetic acid. Metaphase spreads were dropped onto slides, treated with 0.5 mg/mL RNase A (Clontech) for 10 min at 37 °C, stained with 0.5 μg/mL Hoechst (Sigma) for 15 min, and exposed to 5.4×10^3 J/m^2 of 365-nm UV in 2× SSC. BrdU/BrdC-substituted strands were digested with 800 U of Exonuclease III (Promega) for 10 min. Slides were washed with PBS and dehydrated with EtOH. Slides were covered with a hybridization solution containing 100 nM of the Alexa488-TTAGGG probe and then were heated to 90 °C for 5 min and incubated for 2 h. Slides were washed and incubated with hybridization solution containing 100 nM of the Cy3-CCCTAA probe for 2 h and then were washed, DAPI stained, dehydrated with EtOH, and mounted with Prolong Gold.

Telomere Restriction Fragment Analysis. Genomic DNA from MEFs was digested with 4 U/mg of HinfI and RsaI. Samples were separated by pulsed-field gel electrophoresis in 1% wt/vol pulsed-field certified agarose. Gel was washed twice for 15 min with 0.25 M HCl, twice for 15 min each with 0.5 M NaOH and 1.5 M NaCl, and once for 30 min in 0.5 M Tris (pH 7 1.5) and 1.5 M NaCl. Samples were transferred to nylon membrane overnight. DNA was UV-cross-linked to membrane and hybridized at 65 °C with Church buffer [0.5 M $NaPO_4$, 1 mM EDTA (pH 8), 7% (wt/vol) SDS, 1% (wt/vol) BSA] and the ^{32}P-$(CCCTAA)_3$ probe. The blot then was washed and imaged using a PharosFX Plus Molecular Imager (Bio-Rad).

Telomere ChIP. Telomere ChIP was performed as described previously (43).

ACKNOWLEDGMENTS. We thank Titia de Lange, Karlene Cimprich, and Simon Boulton for reagents and Rohit Venkat, Katherine Friedman, Anukana Bhattacharjee, Christopher Kasbek, and Carolyn Price for advice. This work was supported by NIH Grants CA136933 (to D.C.) and CA160432 (to D.C. and C.M.E.). L.A.P. is supported by NIH Grant F31 CA189375 and by NIH Grant T32 GM008554 from the Cellular, Biochemical, and Molecular Sciences Training Program.

1. Flaus A, Martin DM, Barton GJ, Owen-Hughes T (2006) Identification of multiple distinct Snf2 subfamilies with conserved structural motifs. *Nucleic Acids Res* 34(10):2887–2905.
2. Bansbach CE, Bétous R, Lovejoy CA, Glick GG, Cortez D (2009) The annealing helicase SMARCAL1 maintains genome integrity at stalled replication forks. *Genes Dev* 23(20): 2405–2414.
3. Bétous R, et al. (2012) SMARCAL1 catalyzes fork regression and Holliday junction migration to maintain genome stability during DNA replication. *Genes Dev* 26(2):151–162.
4. Ciccia A, et al. (2012) Polyubiquitinated PCNA recruits the ZRANB3 translocase to maintain genomic integrity after replication stress. *Mol Cell* 47(3):396–409.
5. Yusufzai T, Kong X, Yokomori K, Kadonaga JT (2009) The annealing helicase HARP is recruited to DNA repair sites via an interaction with RPA. *Genes Dev* 23(20):2400–2404.
6. Achar YJ, Balogh D, Haracska L (2011) Coordinated protein and DNA remodeling by human HLTF on stalled replication fork. *Proc Natl Acad Sci USA* 108(34):14073–14078.
7. Blastyák A, Hajdú I, Unk I, Haracska L (2010) Role of double-stranded DNA translocase activity of human HLTF in replication of damaged DNA. *Mol Cell Biol* 30(3):684–693.
8. Burkovics P, Sebesta M, Balogh D, Haracska L, Krejci L (2014) Strand invasion by HLTF as a mechanism for template switch in fork rescue. *Nucleic Acids Res* 42(3):1711–1720.
9. MacKay C, Toth R, Rouse J (2009) Biochemical characterisation of the SWI/SNF family member HLTF. *Biochem Biophys Res Commun* 390(2):187–191.
10. Yuan J, Ghosal G, Chen J (2012) The HARP-like domain-containing protein AH2/ZRANB3 binds to PCNA and participates in cellular response to replication stress. *Mol Cell* 47(3):410–421.
11. Yusufzai T, Kadonaga JT (2008) HARP is an ATP-driven annealing helicase. *Science* 322(5902):748–750.
12. Hishiki A, et al. (2015) Structure of a Novel DNA-binding Domain of Helicase-like Transcription Factor (HLTF) and Its Functional Implication in DNA Damage Tolerance. *J Biol Chem* 290(21):13215–13223.
13. Bétous R, et al. (2013) Substrate-selective repair and restart of replication forks by DNA translocases. *Cell Reports* 3(6):1958–1969.
14. Lin JR, Zeman MK, Chen JY, Yee MC, Cimprich KA (2011) SHPRH and HLTF act in a damage-specific manner to coordinate different forms of postreplication repair and prevent mutagenesis. *Mol Cell* 42(2):237–249.
15. Weston R, Peeters H, Ahel D (2012) ZRANB3 is a structure-specific ATP-dependent endonuclease involved in replication stress response. *Genes Dev* 26(14):1558–1572.
16. Yusufzai T, Kadonaga JT (2010) Annealing helicase 2 (AH2), a DNA-rewinding motor with an HNH motif. *Proc Natl Acad Sci USA* 107(49):20970–20973.
17. Ciccia A, et al. (2009) The SIOD disorder protein SMARCAL1 is an RPA-interacting protein involved in replication fork restart. *Genes Dev* 23(20):2415–2425.
18. Postow L, Woo EM, Chait BT, Funabiki H (2009) Identification of SMARCAL1 as a component of the DNA damage response. *J Biol Chem* 284(51):35951–35961.
19. Yuan J, Ghosal G, Chen J (2009) The annealing helicase HARP protects stalled replication forks. *Genes Dev* 23(20):2394–2399.
20. Boerkoel CF, et al. (2002) Mutant chromatin remodeling protein SMARCAL1 causes Schimke immuno-osseous dysplasia. *Nat Genet* 30(2):215–220.
21. Carroll C, et al. (2013) Schimke Immunoosseous Dysplasia associated with undifferentiated carcinoma and a novel SMARCAL1 mutation in a child. *Pediatr Blood Cancer* 60(9):E88–E90.
22. Baradaran-Heravi A, et al. (2012) SMARCAL1 deficiency predisposes to non-Hodgkin lymphoma and hypersensitivity to genotoxic agents in vivo. *Am J Med Genet A* 158A(9):2204–2213.
23. Ghosal G, Yuan J, Chen J (2011) The HARP domain dictates the annealing helicase activity of HARP/SMARCAL1. *EMBO Rep* 12(6):574–580.
24. Mason AC, et al. (2014) A structure-specific nucleic acid-binding domain conserved among DNA repair proteins. *Proc Natl Acad Sci USA* 111(21):7618–7623.
25. Bhat KP, Bétous R, Cortez D (2015) High-affinity DNA-binding domains of replication protein A (RPA) direct SMARCAL1-dependent replication fork remodeling. *J Biol Chem* 290(7):4110–4117.
26. Bansbach CE, Boerkoel CF, Cortez D (2010) SMARCAL1 and replication stress: An explanation for SIOD? *Nucleus* 1(3):245–248.
27. Gilson E, Géli V (2007) How telomeres are replicated. *Nat Rev Mol Cell Biol* 8(10):825–838.
28. Sfeir A, et al. (2009) Mammalian telomeres resemble fragile sites and require TRF1 for efficient replication. *Cell* 138(1):90–103.
29. Bochman ML, Paeschke K, Zakian VA (2012) DNA secondary structures: Stability and function of G-quadruplex structures. *Nat Rev Genet* 13(11):770–780.
30. Griffith JD, et al. (1999) Mammalian telomeres end in a large duplex loop. *Cell* 97(4):503–514.
31. Takai KK, Kibe T, Donigian JR, Frescas D, de Lange T (2011) Telomere protection by TPP1/POT1 requires tethering to TIN2. *Mol Cell* 44(4):647–659.
32. Gong Y, de Lange T (2010) A Shld1-controlled POT1a provides support for repression of ATR signaling at telomeres through RPA exclusion. *Mol Cell* 40(3):377–387.
33. O'Sullivan RJ, et al. (2014) Rapid induction of alternative lengthening of telomeres by depletion of the histone chaperone ASF1. *Nat Struct Mol Biol* 21(2):167–174.
34. Vannier JB, Pavicic-Kaltenbrunner V, Petalcorin MI, Ding H, Boulton SJ (2012) RTEL1 dismantles T loops and counteracts telomeric G4-DNA to maintain telomere integrity. *Cell* 149(4):795–806.
35. Cesare AJ, Reddel RR (2010) Alternative lengthening of telomeres: Models, mechanisms and implications. *Nat Rev Genet* 11(5):319–330.
36. Chung I, Osterwald S, Deeg KI, Rippe K (2012) PML body meets telomere: The beginning of an ALTernate ending? *Nucleus* 3(3):263–275.
37. Bétous R, Glick GG, Zhao R, Cortez D (2013) Identification and characterization of SMARCAL1 protein complexes. *PLoS One* 8(5):e63149.
38. Popuri V, et al. (2014) Human RECQL1 participates in telomere maintenance. *Nucleic Acids Res* 42(9):5671–5688.
39. Henson JD, et al. (2009) DNA C-circles are specific and quantifiable markers of alternative-lengthening-of-telomeres activity. *Nat Biotechnol* 27(12):1181–1185.
40. Svendsen JM, et al. (2009) Mammalian BTBD12/SLX4 assembles a Holliday junction resolvase and is required for DNA repair. *Cell* 138(1):63–77.
41. Muthuswami R, Truman PA, Mesner LD, Hockensmith JW (2000) A eukaryotic SWI2/SNF2 domain, an exquisite detector of double-stranded to single-stranded DNA transition elements. *J Biol Chem* 275(11):7648–7655.
42. Zindy F, et al. (1998) Myc signaling via the ARF tumor suppressor regulates p53-dependent apoptosis and immortalization. *Genes Dev* 12(15):2424–2433.
43. Zimmermann M, Kibe T, Kabir S, de Lange T (2014) TRF1 negotiates TTAGGG repeat-associated replication problems by recruiting the BLM helicase and the TPP1/POT1 repressor of ATR signaling. *Genes Dev* 28(22):2477–2491.